BJP British Journal of Pharmacology

DOI:10.1111/bph.13033
www.brjpharmacol.org

RESEARCH PAPER

S1P-induced airway smooth muscle hyperresponsiveness and lung inflammation *in vivo*: molecular and cellular mechanisms

F Roviezzo[1], R Sorrentino[2], A Bertolino[1], L De Gruttola[1], M Terlizzi[2], A Pinto[2], M Napolitano[3], G Castello[3], B D'Agostino[4], A Ianaro[1], R Sorrentino[1] and G Cirino[1]

[1]*Dipartimento di Farmacia, Università di Napoli Federico II, Napoli, Italy,* [2]*Dipartimento di Farmacia, Università di Salerno, Salerno, Italy,* [3]*National Cancer Institute 'G. Pascale Foundation', OncologyResearch Center of Mercogliano (CROM), Mercogliano, Italy, and* [4]*Dipartimento di Medicina Sperimentale, Sezione di Farmacologia L. Donatelli, Seconda Università degli Studi di Napoli, Naples, Italy*

Correspondence
Giuseppe Cirino, Department of Pharmacy, University of Naples Federico II, Via Domenico Montesano 49, Napoli 80132, Italy. E-mail: cirino@unina.it

Received
6 December 2013
Revised
24 November 2014
Accepted
27 November 2014

BACKGROUND AND PURPOSE

Sphingosine-1-phosphate (S1P) has been shown to be involved in the asthmatic disease as well in preclinical mouse experimental models of this disease. The aim of this study was to understand the mechanism(s) underlying S1P effects on the lung.

EXPERIMENTAL APPROACH

BALB/c, mast cell-deficient and Nude mice were injected with S1P (s.c.) on days 0 and 7. Functional, molecular and cellular studies were performed.

KEY RESULTS

S1P administration to BALB/c mice increased airway smooth muscle reactivity, mucus production, PGD_2, IgE, IL-4 and IL-13 release. These features were associated to a higher recruitment of mast cells to the lung. Mast cell-deficient Kit $^{W\text{-}sh/W\text{-}sh}$ mice injected with S1P did not display airway smooth muscle hyper-reactivity. However, lung inflammation and IgE production were still present. Treatment *in vivo* with the anti-CD23 antibody B3B4, which blocks IgE production, inhibited both S1P-induced airway smooth muscle reactivity *in vitro* and lung inflammation. S1P administration to Nude mice did not elicit airway smooth muscle hyper-reactivity and lung inflammation. Naïve (untreated) mice subjected to the adoptive transfer of CD4+ T-cells harvested from S1P-treated mice presented all the features elicited by S1P in the lung.

CONCLUSIONS AND IMPLICATIONS

S1P triggers a cascade of events that sequentially involves T-cells, IgE and mast cells reproducing several asthma-like features. This model may represent a useful tool for defining the role of S1P in the mechanism of action of currently-used drugs as well as in the development of new therapeutic approaches for asthma-like diseases.

Abbreviations

CFSE, carboxyfluoresceindiacetate, succinimidyl ester; FcεRI, high affinity IgE receptor; H&E, haematoxylin and eosin; PAS, periodic acid/Alcian blue/Schiff; S1P, sphingosine-1-phosphate; SPK, sphingosine kinase

Tables of Links

TARGETS	
GPCRs[a]	**Enzymes**[b]
S1P receptors	Sphingosine kinase (SPK)

LIGANDS	
Carbachol	IL-13
IL-4	PGD_2
IL-6	RANTES (CCL5)

These Tables list key protein targets and ligands in this article which are hyperlinked to corresponding entries in http://www.guidetopharmacology.org, the common portal for data from the IUPHAR/BPS Guide to PHARMACOLOGY (Pawson *et al.*, 2014) and are permanently archived in the Concise Guide to PHARMACOLOGY 2013/14 ([a,b]Alexander *et al.*, 2013a,b).

Introduction

Sphingosine-1-phosphate (S1P) is a bioactive sphingolipid metabolite with pleiotropic actions that mediates several biological functions of many cell types (Pyne and Pyne, 2000; 2002; Spiegel and Milstien, 2003). S1P, produced following the activation of sphingosine kinases (SPK), exerts most of its effects binding five distinct GPCRs designated as $S1P_{1-5}$ (Pyne and Pyne, 2000; Spiegel and Milstien, 2003). High levels of S1P have been found in the broncho-alveolar lavage of asthmatic patients and they are directly correlated to eosinophil count (Ammit *et al.*, 2001). Therefore, S1P has been thought to be involved in asthma (Oskeritzian *et al.*, 2007; Ryan and Spiegel, 2008; Lai *et al.*, 2011).

S1P aggravates antigen-induced airway inflammation in mice (Chiba *et al.*, 2010) and increases sensitivity to methacholine (Kume *et al.*, 2007; Price *et al.*, 2012). Airway smooth muscle cells stimulated with S1P release high levels of RANTES and IL-6, which play a critical role in the lung (Ammit *et al.*, 2001; Roviezzo *et al.*, 2004; Jenkins *et al.*, 2011). In humans, it has been shown that mast cells obtained from the airways of allergic patients produce high levels of S1P that are associated with mast cell chemotaxis, degranulation, cytokine and lipid mediator production (Olivera, 2008; Rivera *et al.*, 2008). These findings have been confirmed by several preclinical studies showing that S1P is pivotal in IgE-mediated mast cell degranulation and secretion of pro-inflammatory cytokines. Particular relevant in this context is the finding that the ligation of FcεRI, the high-affinity IgE receptor, induces SPK activation and consequently the secretion of S1P by mast cells (Olivera and Rivera, 2011). In this context, we previously demonstrated that treatment with a non-selective inhibitor of SPKs significantly inhibits ovalbumin-induced hyper-reactivity (Roviezzo *et al.*, 2007). In addition, we have also shown that s.c. administration of S1P by itself, in the absence of sensitization and airway challenge, induces airway smooth muscle hyper-reactivity associated with an increase in lung Th_2 cytokines in a time- and dose-dependent manner (Roviezzo *et al.*, 2010).

The aim of this study was to understand the mechanism(s) underlying to the effects of S1P on the lung. Our study has been conducted by administering S1P to BALB/c, mast cell-deficient and Nude mice and performing molecular and functional analysis.

Methods

Mice

BALB/c, mast cell-deficient Kit $^{W\text{-}sh/W\text{-}sh}$ (Tono *et al.*, 1992; Berrozpe *et al.*, 1999), BALB/c-Nude mice were purchased from Charles River (Milan, Italy). The animals were housed in a controlled environment and provided with standard rodent chow and water. All mouse strains (20–25 g) were housed with a 12 h light–dark cycle and were allowed food and water *ad libitum*. The total number of mice used was 516. Animal care was in compliance with Italian regulations on protection of animals used for experimental and other scientific purposes (D. M. 116192) as well as with the EEC regulations (O. J. of E. C. L 358/1 12/18/1986). All studies were performed in accordance with European Union regulations for the handling and use of laboratory animals and approved by the local committee and are reported in accordance with the ARRIVE guidelines for reporting experiments involving animals (Kilkenny *et al.*, 2010; McGrath *et al.*, 2010).

S1P exposure

BALB/c, mast cell-deficient (Kit $^{W\text{-}sh/W\text{-}sh}$) or Nude mice received a s.c. injection of 0.1 mL of S1P (10 ng; Enzo Life Science, Rome, Italy) dissolved in sterile saline containing BSA (0.001%) according to the manufacturer's instructions. Briefly, S1P was dissolved in sterile saline containing BSA, fatty acid free, at the concentration of 1 mg·mL^{-1}. The stock solution obtained was used to perform the serial dilution in sterile saline. Therefore when S1P was administered, the final concentration of BSA was 0.001%. S1P was administered on days 0 and 7 (Figure 1A). The vehicle used in the experimental procedures contained 0.001% of BSA. Mice were killed on days 7, 14 or 21. Mice were anaesthetized before being killed.

Bronchial tissues were rapidly dissected and cleaned from fat and connective tissue. Isolated bronchi and lungs were then utilized for functional and molecular studies.

In another set of experiments, mice received the purified rat Anti-Mouse CD23 monoclonal Ab (10 μg per mouse; B3B4 clone, anti-CD23; BD Pharmingen, DBA, Milan, Italy) 30 min before S1P administration. Each experimental group consisted of 6–8 mice.

Airway responsiveness measurements

Mice were killed and bronchial tissues were rapidly dissected and cleaned of fat and connective tissue. Rings, 1–2 mm long,

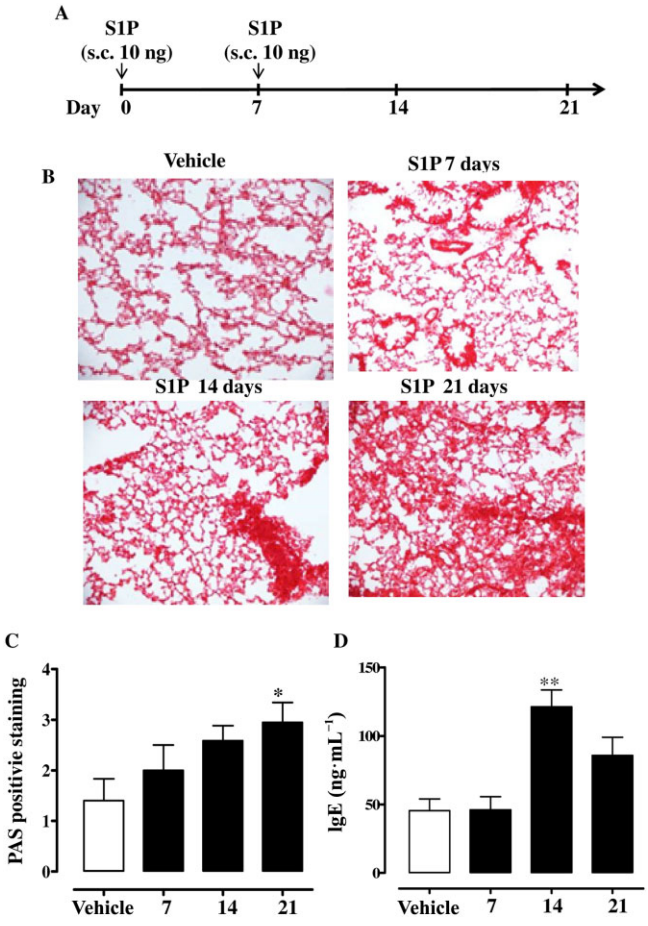

Figure 1

Systemic S1P administration induces lung inflammation. (A) Mice received S1P (10 ng) or vehicle (BSA 0.001%), s.c., on days 0 and 7. (B) Lung sections were fixed and stained with H&E. Lung sections were photographed under light microscopy at ×10 magnification. (C) PAS was performed to detect glycoprotein (*$P < 0.05$ vs. vehicle). (D) Sera were collected and levels of total IgE were determined by using specific ELISA (**$P < 0.01$ vs. vehicle). Data are means ± SEM $n = 6$ mice in each group.

were cut and placed in organ baths mounted to isometric force transducers (Type 7006, Ugo Basile, Comerio, Italy) and connected to a Powerlab 800 (AD Instruments, Ugo Basile, Comerio, Italy). Rings were initially stretched until a resting tension of 0.5 g was reached and allowed to equilibrate for at least 30 min. In each experiment, bronchial rings were challenged with carbachol (10^{-6} mol·L^{-1}) until the response was reproducible. Once a reproducible response was achieved, bronchial reactivity was assessed performing a cumulative concentration-response curve to carbachol (1×10^{-8}–3×10^{-5} mol·L^{-1}).

Flow cytometry analysis

Lungs were isolated and digested with 1 U·mL^{-1} collagenase (Sigma Aldrich, Milan, Italy). Cell suspensions were passed through 70 µm cell strainers, and red blood cells were lysed. Cell suspensions were used for flow cytometric analysis of different cell subtypes (Sorrentino *et al.*, 2008; 2011). The composition of lung inflammatory cells was determined by flow cytometry (BD FacsCalibur Milan, Italy) using the following antibodies: CD11c-APC, CD11b-PeCy5.5, cKit-PeCy5.5 or -PE, IgE-FITC (Bioscience, San Diego, CA, USA). The different lymphocyte populations in the proximal lymph nodes were discriminated by means of anti-CD4-Pe, anti-CD8PerCP, anti-CD45R APC antibodies (eBioscience, San Diego, CA, USA). Appropriate isotype controls were used.

In a separate set of experiments, mediastinic lymph nodes were digested (collagenase 0.5 U·mL^{-1}) and CD4+ T-cells were isolated by using immunomagnetic beads for negative selection (Rega *et al.*, 2013) according to the manufacturer's instructions (EasySep, Voden, Milan, Italy). The purity of CD4+ T-cells was around ~90%. CD4+ T-cells were then marked for carboxyfluoresceindiacetate, succinimidyl ester (CFSE; 5 µM; Molecular Probes, Invitrogen, Milan, Italy) to perform proliferation assay by using CD3/CD28 stimulation (CD3/CD28 beads, Invitrogen, Milan, Italy). CFSE flow cytometry data were analysed by means of ModFit software (BD Pharmingen).

In another set of experiments, CD4+ T-cells harvested from vehicle-, S1P- or S1P+ anti-CD23-treated mice were adoptively transferred into naïve (untreated mice). Then 1×10^6 CD4+ T-cells were injected i.v. as described previously (Rega *et al.*, 2013).

Immunohistochemistry

Left lung lobes were fixed in OCT medium (Pella Inc., Milan, Italy) and 7 µm cryosections were cut. The degree of inflammation was scored by blinded observers by using haematoxylin and eosin (H&E) and periodic acid/Alcian blue/Schiff staining (PAS). PAS Staining (Sigma Aldrich, Milan Italy) was performed according to the manufacturer's instructions to detect glycoprotein. PAS+ cryosections were graded with scores 0 to 4 to describe low to severe lung inflammation as follows: 0: <5%; 1: 5–25%; 2: 25–50%; 3: 50–75%; 4: <75% positive staining/total lung area. Immunohistochemical detection of CD23 was performed by using anti-CD23 or rat IgG isotype control. The diamino-benzidinic acid system was used to detect complexes. Positive staining was quantified by means of Image J software (NIH, Baltimore, MD, USA) and expressed as CD23 positive staining compared with the total area of the lung section. At least five sections were considered for each animal and the mean of the positive staining compared with the total area were plotted.

Measurement of serum IgE and PGD_2 levels

Blood was collected from the heart. Total serum IgE levels were measured by means of ELISA using matched antibody pairs (BD Pharmingen, Franklin Lakes, NJ, USA). The amount of PGD_2 was quantified using an EIA Kit (Cayman, Ann Arbor, MI, USA).

Cytokine measurements

Pulmonary IL-4 (R&D System, London, UK) and IL-13 (eBioscience, San Diego, CA, USA) were determined by ELISA.

Statistical analysis

Data are means ± SEM from at least six mice in each group. The level of statistical significance was determined by two-

way ANOVA followed by Bonferroni's test for multiple comparisons or Student's *t*-test by using the Graph Pad Prism software, when appropriate.

Results

S1P induces airway smooth muscle hyper-reactivity and lung inflammation

Lungs harvested from mice injected with S1P (Figure 1A) displayed a progressive alteration in lung morphology. The effect was maximal at 21 days after S1P challenge (Figure 1B) and was associated with increased mucus production as determined by PAS staining (Figure 1C). Plasma levels of IgE (Figure 1D) were significantly increased too. Flow cytometry analyses of lungs showed a significant increase in the percentage of mast cells, identified as CD11c+cKit+IgE+ cells (Figure 2A and Figure 2B). Mast cells were stained for IgE since they covalently bind to its receptor (FcεRI) on these cells (Metzger, 1991). Plasma levels of PGD_2 were significantly increased in S1P-treated compared with vehicle-treated mice (Figure 2C).

S1P-induced hyper-reactivity, but not lung inflammation, is attenuated in mast cell-deficient Kit $^{W\text{-}sh/W\text{-}sh}$ mice

In mast cell-deficient Kit $^{W\text{-}sh/W\text{-}sh}$ mice S1P failed to induce bronchial hyper-responsiveness (Figure 3A). Conversely, lungs harvested from the same animals still displayed (i) altered alveolar structure and (ii) increased mucus production (Figure 3B and 3C) in comparison with wild type. Basal serum IgE was significantly reduced in Kit $^{W\text{-}sh/W\text{-}sh}$ mice when compared with wild-type mice (Figure 3D). Nevertheless, S1P challenge significantly increased IgE levels in Kit $^{W\text{-}sh/W\text{-}sh}$ mice when compared with the basal levels of mast cell-deficient mice (Figure 3D).

S1P induces lung inflammation and airway smooth muscle hyper-reactivity in an IgE-dependent manner

CD23 is an important regulatory receptor for IgE production and its interaction with IgE can amplify IgE-associated immune responses (Morris *et al.*, 1994; Cheng *et al.*, 2010; Galli and Tsai, 2012). Immunohistochemical analysis (Figure 4A) showed that CD23 expression was significantly increased in S1P-treated mice with a maximal effect at 21 days after S1P challenge in comparison with vehicle mice (Figure 4B). Therefore, in order to investigate the role of IgE in S1P-induced airway dysfunction, we used an anti-CD23 monoclonal antibody, B3B4. Administration of anti-CD23 *per se* did not affect S1P-induced increase in pulmonary mast cell infiltration (Figure 4C). Conversely, anti-CD23 significantly reduced S1P-induced IgE increase (Figure 4D) thereby confirming the role of CD23 in S1P-induced IgE production.

IL-4 and IL-13 are key cytokines for the initiation of Th2-mediated responses and for IgE isotype class switching (Finkelman *et al.*, 1990; Zurawski and de Vries, 1994). As shown in Figure 4E and 4F, S1P administration induced a significant increase in both IL-4 (Figure 4E) and IL-13 (Figure 4F) in the lung. Anti-CD23 inhibited S1P-induced expression of IL-13 (Figure 4F), but not of IL-4 (Figure 4E).

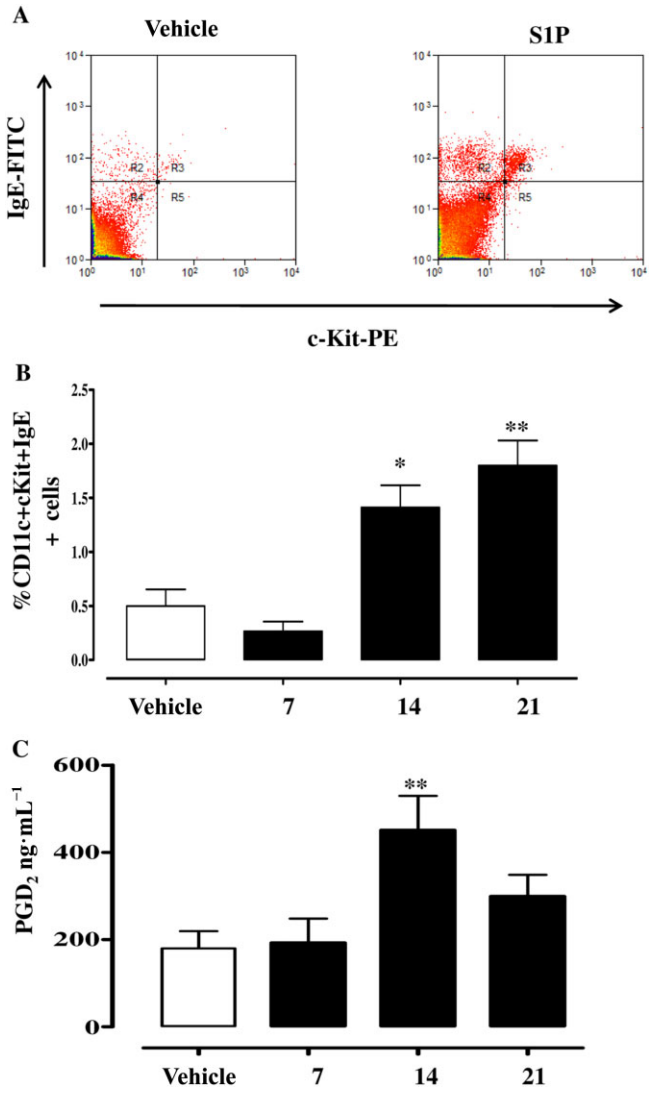

Figure 2

S1P increases mast cell infiltration in the lung. (A) Mast cells were identified as IgE+cKit+ cells by flow cytometry as shown in the representative dot plot. (B) Mast cell infiltration was quantified after 7, 14 and 21 days following S1P administration. (C) Sera were collected and PGD_2 levels were determined by using specific ELISA. $^*P < 0.05$, $^{**}P < 0.01$ versus vehicle. Data are means ± SEM $n = 6$ mice in each group.

However, the administration of anti-CD23 to S1P-treated mice prevented airway smooth muscle hyper-responsiveness (Figure 5A), lung damage (Figure 5B) and mucus production (Figure 5C).

T-cells are involved in S1P-induced effects on lung

The major control step in IgE synthesis is the regulation of IgE class-switch recombination, which is mostly T-cell

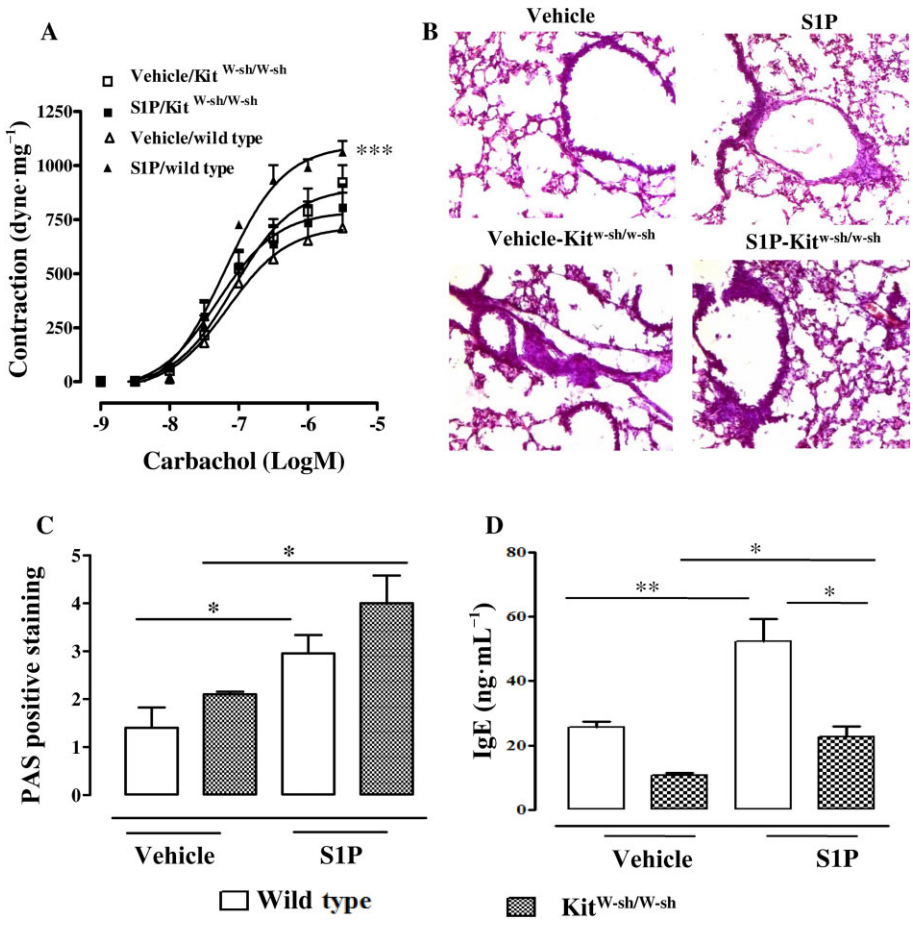

Figure 3

Mast cells are essential for the development of S1P-induced bronchial hyper-reactivity, but not for lung inflammation. Mast cell-deficient Kit $^{W\text{-}sh/W\text{-}sh}$or wild-type mice received S1P (10 ng) or vehicle (BSA 0.001%) s.c. on days 0 and 7. Mice were killed on day 21. (A) Assessment of bronchial reactivity to carbachol (***$P < 0.001$ vs. vehicle). (B) Lung sections were fixed and stained with PAS (*$P < 0.05$). Lung sections were photographed under light microscopy at ×10 magnification. (C) PAS staining was quantified as described in Methods. (D) Sera were collected and levels of IgE were determined by ELISA (*$P < 0.05$; **$P < 0.01$). Data are means ± SEM $n = 6$ mice in each group.

dependent (Geha *et al.*, 2003; Rosenwasser, 2011). Our data define IgE/CD23 signalling as a key driver for the effects triggered by S1P in the airways. In order to extend our observations on the role of CD23 and to further elucidate the role of IgE-dependent mechanisms, we evaluated T-cell involvement. Nude mice injected with S1P did not develop bronchial hyper-responsiveness (Figure 6A). In addition, alteration of lung structure (Figure 6B), mucus production (Figure 6C) and mast cell infiltration (Figure 6D) in S1P-treated Nude mice were significantly lower than wild-type mice. Plasma levels of IgE were unaltered by S1P in Nude mice compared with wild type (Figure 6E). Accordingly, we observe neither an increase in CD23 pulmonary expression (Figure 6F), nor IL-4/IL-13 over-expression in the lung (data not shown).

Adoptive transfer of S1P-derived CD4+ T-cells into naïve mice induces airway smooth muscle hyper-reactivity and lung inflammation

In order to gain further insight into the cellular mechanisms, we isolated CD4+ T-cells. CD4+ T-cells were labelled at day 0 with CFSE (parent histogram; Figure 7A) and then cultured for 3 days in the presence or absence of CD3/CD28 beads. CD4+ T-cells were isolated from the mediastinic lymph node of vehicle- (Figure 7B and 7C), S1P- (Figure 7D and 7E), IgG- (Figure 7F), anti-CD23 (Figure 7G and 7H) or S1P+ anti-CD23- (Figure 7I and 7J) treated mice. CD4+ T-cells harvested from S1P-treated mice (Figure 7E) displayed a basal increase in the proliferation rate as compared with vehicle-treated mice (Figure 7C), even in the absence of CD3/CD28 beads (Figure 7B and 7D; Supporting Information Fig. S1). We observed that CFSE+ CD4+ T-cells proliferated for up to seven generations when they were obtained from S1P- (Figure 7D and 7E), but not vehicle-treated mice (Figure 7B and 7C). The proliferation rate of CD4+ T-cells induced by S1P was not affected by anti-CD23 treatment (Figure 7I and 7J, Supporting Information Fig. S1). IgG- (Figure 7F, Supporting Information Fig. S1) or anti-CD23- (Figure 7G and 7H, Supporting Information Fig. S1) derived CD4+ T-cells did not show any significant increase in the proliferation rate (Supporting Information Fig. S1). These results imply that the role of CD23 *in vivo* is to regulate

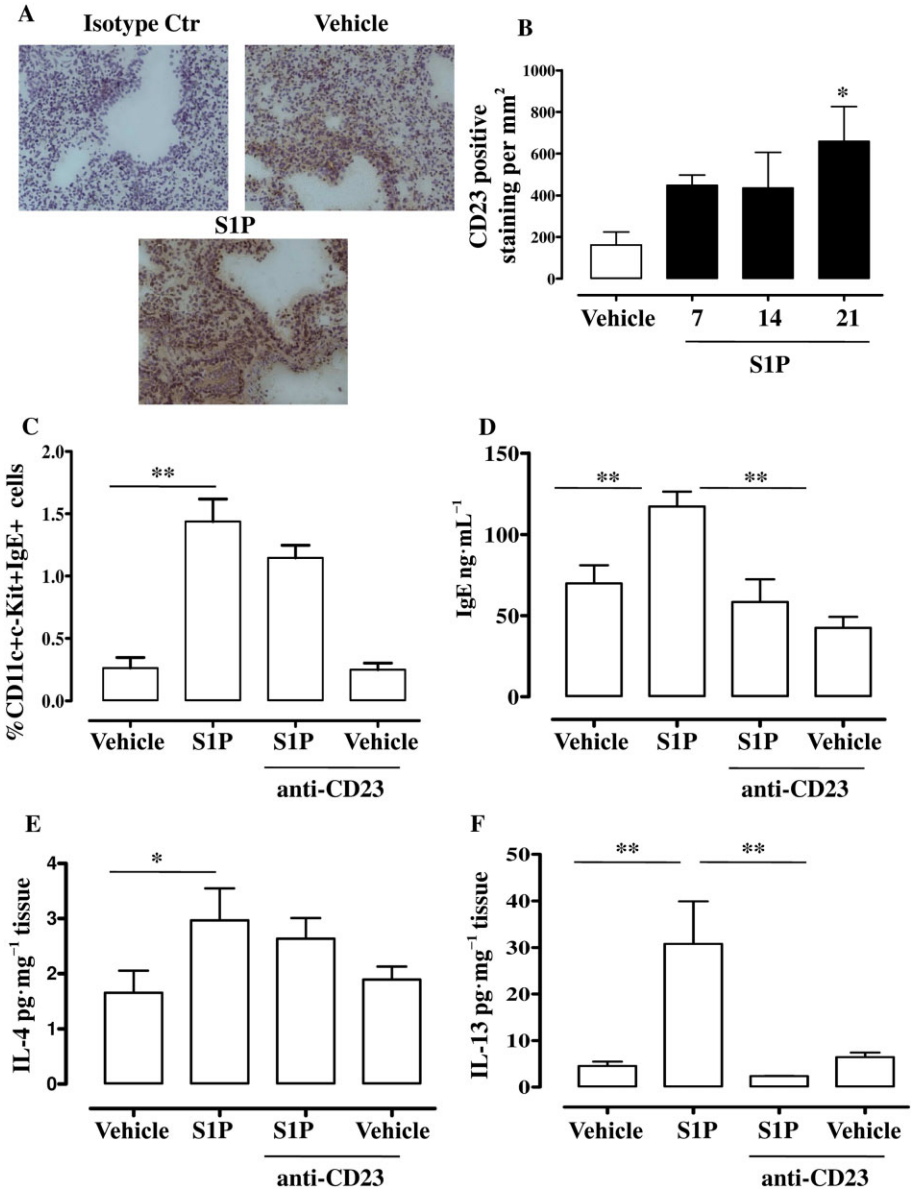

Figure 4

S1P enhances pulmonary CD23 (FcRII) expression. (A) Immunohistochemical detection of CD23 was performed on lung sections harvested from mice challenged with vehicle or S1P by using anti-CD23 monoclonal Ab (B3B4, anti-CD23) or rat IgG isotype control as shown in the representative lung section staining. Lung sections were photographed under light microscopy at ×10 magnification. (B) CD23 quantification was performed at 7, 14 and 21 days after S1P challenge (*$P < 0.05$ vs. vehicle). In another set of experiments, anti-CD23 (B3B4; 10 μg per mice) was administered i.p. 30 min before S1P or vehicle on days 0 and day 7. On day 21, mice were killed. (C) Pulmonary mast cells were identified as IgE+cKit+ cells by flow cytometry (**$P < 0.01$). (D) Sera were collected to determine IgE levels by ELISA (**$P < 0.01$); (E, F) pulmonary expression of IL-4 (*$P < 0.05$) and IL-13 (**$P < 0.01$) was determined by ELISA. Data are means ± SEM $n = 6$ mice in each group.

negatively IgE production during S1P exposure without a direct significant effect on T-cell growth or differentiation. These latter data fit well with the lack of effect of anti-CD23 in regulating IL-4 expression.

To determine whether S1P could directly affect the proliferation of CD4+ T-cells, we incubated CD4+ T-cells obtained from vehicle-treated mice with S1P. In these experimental conditions, there was no detectable increase in the proliferation index (data not shown).

Finally, adoptive transfer of CD4+ T-cells, harvested from the mediastinic lymph node of S1P-treated mice, into naïve mice was performed. S1P-derived CD4+ T-cell adoptively transferred into naïve mice increased mast cell infiltration (Figure 8A), bronchial reactivity (Figure 8B), lung inflammation (Figure 8C), IL-4 (Figure 8D) and IL-13 (Figure 8E) release. Conversely, adoptive transfer of CD4+ T-cells, harvested from mice treated with anti-CD23 and S1P reversed airway smooth muscle hyper-reactivity (Figure 8B), lung

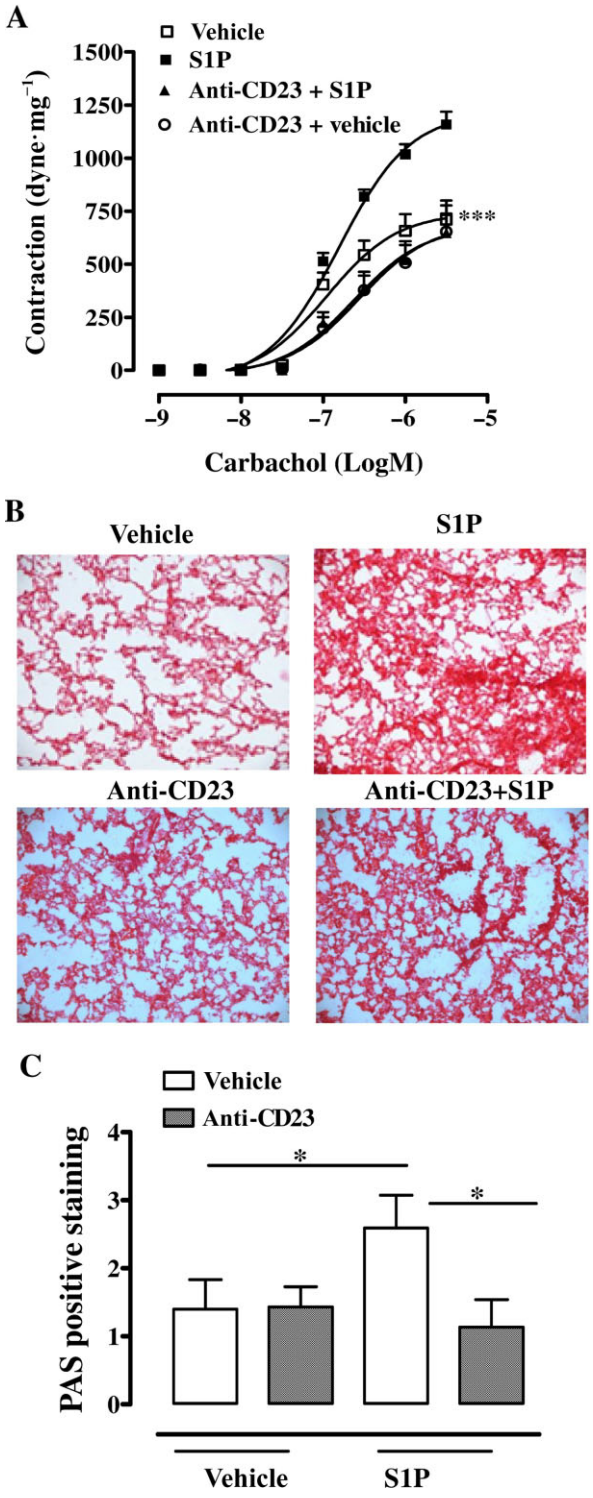

Figure 5

Anti-CD23 (B3B4) attenuates S1P-mediated effects on the lung. Anti-CD23 (B3B4; 10 μg per mice) was administered i.p. 30 min before S1P on days 0 and 7. Mice were killed on day 21. (A) Bronchial responses to carbachol were evaluated (***$P < 0.001$ vs. S1P). (B) Representative staining of lung sections with H&E. (C) Quantification of PAS staining performed as described in Methods (*$P < 0.05$). Lung sections were photographed under light microscopy at ×10 magnification. Data are means ± SEM $n = 6$ mice in each group.

inflammation (Figure 8C) and IL-13 upregulation (Figure 8E). In agreement with previous data (Figure 4), neither mast cell infiltration (Figure 8A) nor IL-4 up-regulation (Figure 8D) were modified.

Discussion and conclusions

In our previous studies, we showed lower bronchial reactivity and lung inflammation after the inhibition of sphingosine kinases in ovalbumin-sensitized mice. Here we showed that s.c. administration of S1P in the absence of an allergen causes a progressive alteration in pulmonary parenchyma morphology, an increased mucus production, lung inflammation and higher bronchial reactivity. These morphological and functional changes were preceded by an increase in plasma levels of PGD_2 and IgE and lung IL-4 and IL-13.

A large body of evidence suggests that both IgE and mast cells are key factors for the pathophysiological changes and tissue remodelling associated with chronic allergic inflammation in asthma. Such effects include IgE-dependent regulation of mast cells, mast cell-independent IgE-mediated actions and mast cell activities that do not directly involve IgE. In order to understand the possible involvement of these mechanisms in our model, we treated mast cell KO (Kit $^{W\text{-}sh/W\text{-}sh}$) mice with S1P. In Kit $^{W\text{-}sh/W\text{-}sh}$ mice, S1P did not cause airway smooth muscle hyper-reactivity. However, lung inflammation, as defined by mucus production and IgE levels, was still evident. Thus, the absence of mast cells does not affect IgE levels suggesting an alternative target for IgE in our mouse model.

CD23 is the low-affinity receptor for IgE and has been implicated in a number of inflammatory conditions, and is considered to be important in the regulation of IgE production. An altered expression of CD23 has been widely associated with allergic diseases (Morris *et al.*, 1994; Rosenwasser and Meng, 2005; Cheng *et al.*, 2010). Based on these notions, we found that lung CD23 expression was significantly increased in S1P-treated compared with vehicle mice. In order to define CD23's role, we treated mice with a neutralizing antibody (B3B4 clone), extensively characterized for its high affinity for CD23 and for a reciprocal inhibitory pattern with IgE. Indeed, treatment of mice with the anti-CD23 and S1P reduced airway smooth muscle hyper-responsiveness, pulmonary hyperplasia, IL-13 and IgE levels, but pulmonary mast cell infiltration and IL-4 levels were not altered. Therefore, these data, taken together with previous evidence, imply that S1P/CD23 signalling is not directly involved in mast cell recruitment, but rather interferes with their activation, as suggested by the marked reduction in production of IgE. This hypothesis is also supported by the reduced levels of IL-13 after anti-CD23 treatment. Similarly, we did not observe any change in IL-4 release after the treatment with anti-CD23, suggesting a predominant Th2 bias in S1P-induced asthma-like model in mice.

Therefore, in order to further gain insight into the cellular mechanisms, S1P was injected in Nude mice, which lack a functional adaptive immunity. In Nude mice, S1P did not elicit bronchial hyper-responsiveness, pulmonary infiltration of mast cells and IgE production. These features were coupled to a lack of induction of both cytokines IL-4 and IL-13 as well

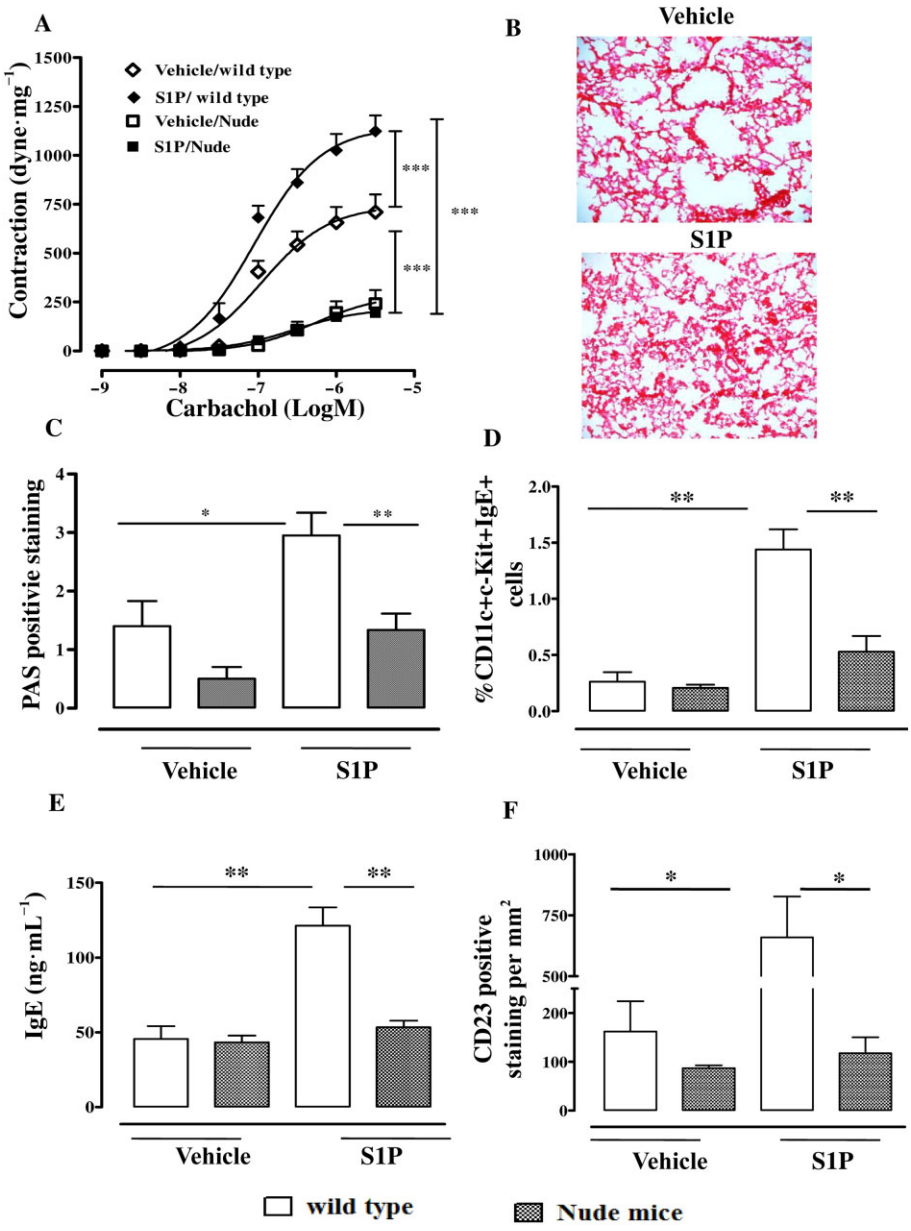

Figure 6

T-cell plays a key role in S1P-mediated effects on lung. Nude athymic mice or wild-type mice received S1P (10 ng) or vehicle (BSA 0.001%) s.c. on days 0 and 7. Mice were killed on day 21. (A) Assessment of bronchial response to carbachol (***$P < 0.001$). (B) Representative staining of lung sections with H&E. (C) Quantification of PAS staining performed as described inMethods (*$P < 0.05$, **$P < 0.01$). (D) Pulmonary mast cells quantified by flow cytometry (**$P < 0.01$). (E) Sera IgE levels determined by ELISA (**$P < 0.01$). (F) Immunhistochemical detection of CD23 (*$P < 0.05$) on lung sections by using anti-CD23 monoclonal Ab (B3B4). Data are means ± SEM $n = 6$ mice in each group.

as of CD23 in the lung. Thus, T-cells, opposite to mast cells, trigger the functional, molecular and cellular changes elicited by S1P. Thus, both IgE-dependent pathways and Th2-like bias orchestrated S1P-induced asthmatic conditions in mice.

The idea that all these events are T-cell dependent is further sustained by the finding that the CD4+ T lymphocytes, harvested from BALB/c mice exposed to S1P, showed an increased ability to proliferate *in vitro*. To note, CD4+ T-cells harvested from S1P-treated mice were able to proliferate even in the absence of the *in vitro* stimulation with CD3/CD28 beads. However, the proliferation rate of CD4+ T-cells, obtained from mice pretreated *in vivo* with the anti-CD23 before S1P administration, was not altered. This indicates that the major action of CD23 *in vivo* is to negatively regulate IgE production without a significant effect on T-cell growth or differentiation. These data fit well with the lack of effect of anti-CD23 in regulating IL-4 release, mainly involved, together with IL-13, IgE and PGD_2 (Bice *et al.*, 2014), in a Th2 skew in the lung of S1P-treated mice. That these mechanisms, triggered by S1P, require this *in vivo* cellular activation is

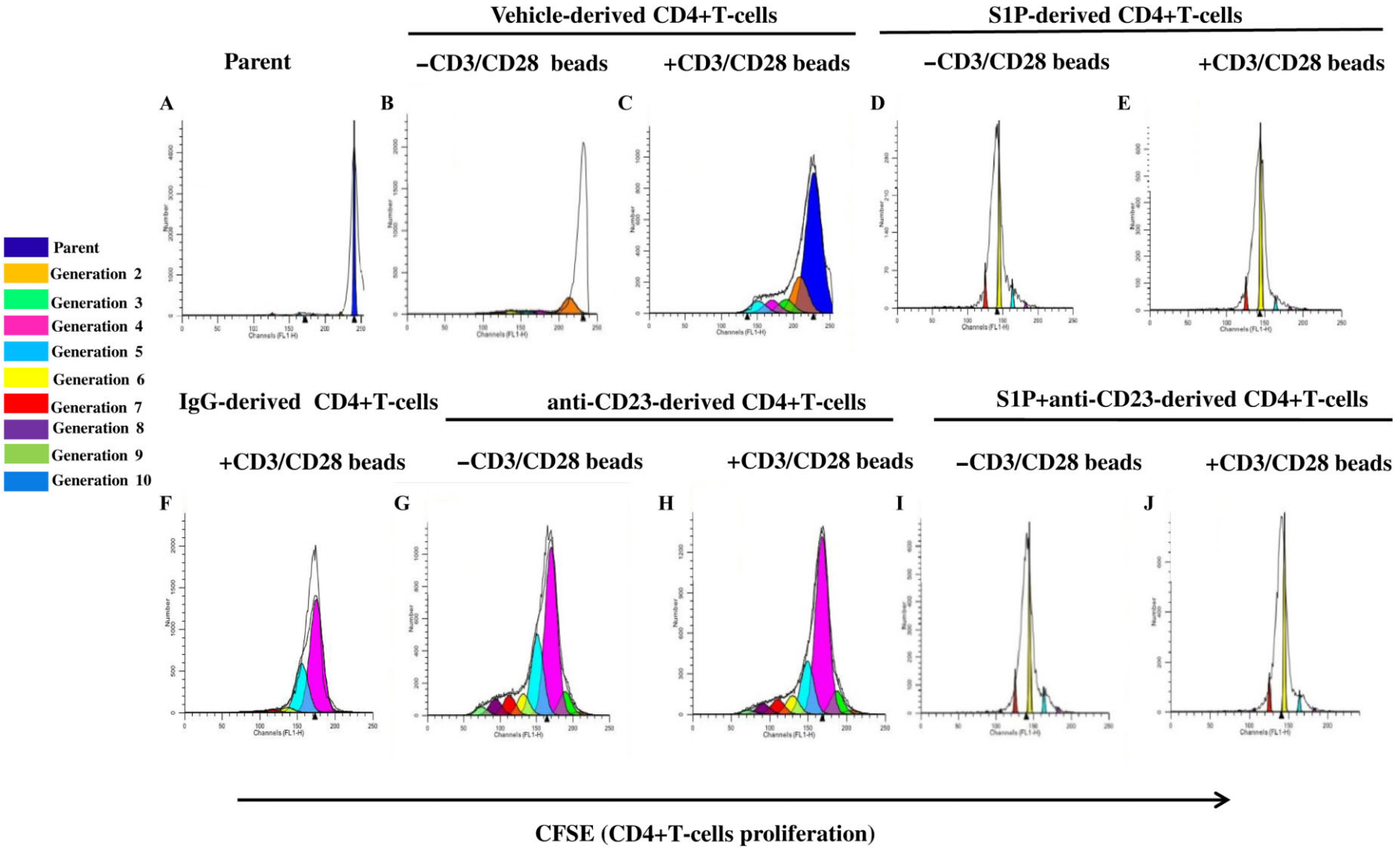

Figure 7

Lymphocytes harvested from S1P-treated BALB/c mice have an increased ability to proliferate. CD4+ T-cells were isolated from the mediastinic lymph node of vehicle-, S1P-, IgG- or S1P+ anti-CD23-treated mice. CD4+ T-cells were labelled on day 0 with CFSE (parent histogram – A) and then cultured for 3 days in the presence (C, E, F H, J) or absence (B, D, G, I) of CD3/CD28 beads. Histograms in panels B to J represent the proliferation of CD4+ T-cells isolated from the lymph node of vehicle- (B and C), S1P- (D and E), IgG- (F), anti-CD23- (G and H) and S1P+ anti-CD23- (I and J) treated mice. Experiments were performed at three different experimental times. The histograms reported are representative. Data were analysed by means of ModFlt3 program (BD FACSCalibur).

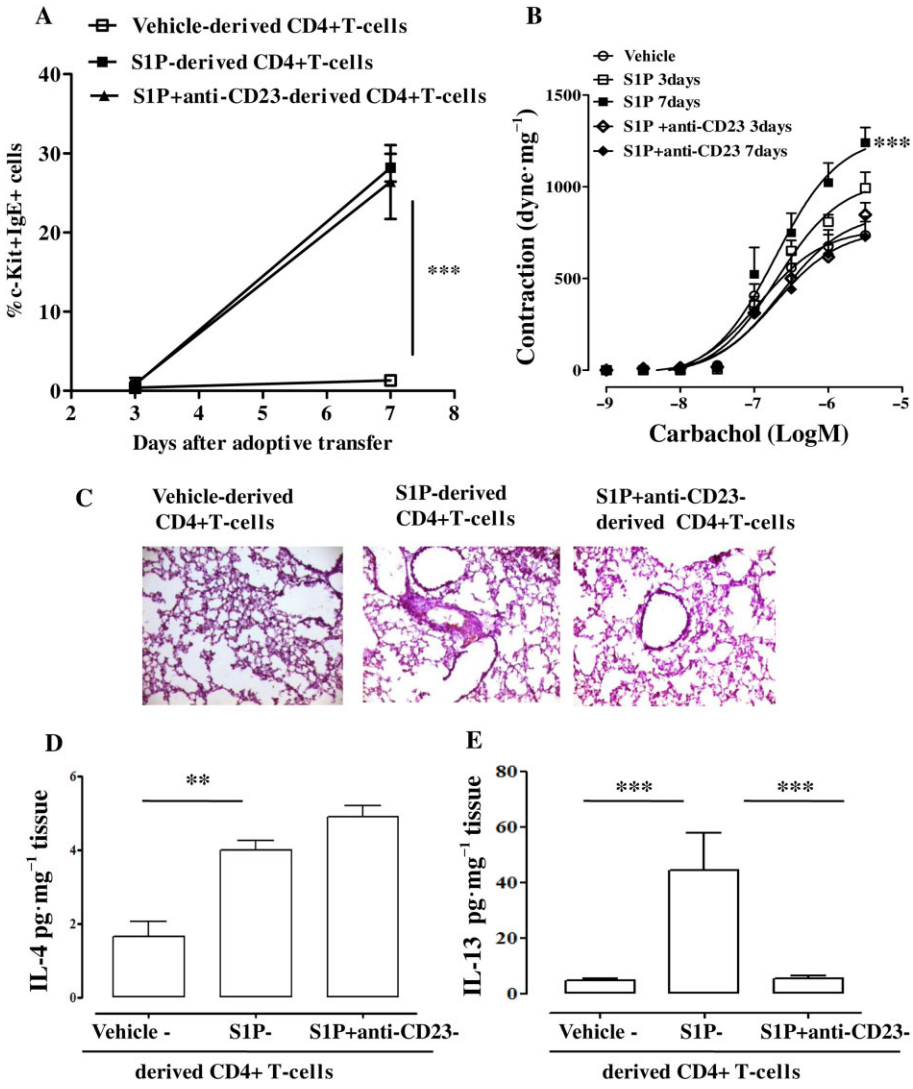

Figure 8

Adoptive transfer of CD4+ cells from S1P-treated mice into naïve (untreated) mice mimics S1P-induced effects in BALB/c mice. Adoptive transfer of CD4+ T-cells derived from vehicle-, S1P- or anti-CD23+ S1P-treated mice into naïve BALB/c mice was performed. Mice were killed at 3 and 7 days following adoptive transfer. (A) Mast cells identified as CD11c+cKit+IgE+ cells by flow cytometry. (B) Assessment of bronchial response to carbachol. (C) PAS staining of lung sections harvested from mice after 7 days of adoptive transfer. (D) Pulmonary levels of IL-4 (**$P < 0.01$). (E) Pulmonary levels of IL-13 (***$P < 0.001$). Data are means ± SEM $n = 6$ mice in each group.

strongly supported by the finding that CD4+ T-cells, harvested from vehicle-treated mice, were not able to proliferate when exposed *in vitro* to S1P. These latter events occur in an IgE-independent manner.

To further confirm that S1P induces a modulation of the adaptive response, we performed adoptive transfer experiments. S1P-derived CD4+ T-cells adoptively transferred into naïve mice increased mast cell infiltration, bronchial reactivity pulmonary inflammation, IL-4 and IL-13 release. As expected, adoptive transfer of CD4+ T-cells derived from S1P-treated mice receiving anti-CD23 into naïve mice did not promote any effect on the lung. In particular, we did not observe any increase in airway smooth muscle reactivity or an inflammatory response. Conversely, IL-4 over-expression was still present. These data, together with the studies performed in mast cell KO and Nude mice, confirm that CD4+ T-cells are the main cells involved in S1P-induced effects. In addition, this implies an obligatory role for CD23/IgE signalling to trigger IgE-mediated immune responses in order to observe functional changes in the lung. However, the role of innate immune cells in this context still remains to be elucidated.

In conclusion, systemic administration of S1P triggers a cascade of events that sequentially involves T-cells, IgE and mast cells, which leads to the asthma-like symptoms in mice. Therefore, the model described and characterized in this study may represent a useful tool to define the role of S1P in the mechanism of action of currently-used drugs, as well as in the development and characterization of new therapeutic approaches.

Acknowledgements

This work has been financially supported by the project PRIN 2009. R. Sorrentino was supported by a fellowship from Programma Operativi Nazionali (PON) MODO.

Author contributions

F. R. and G. C. conceived and designed the experiments and wrote the manuscript; L. D G and A. B. performed functional experiments of bronchial reactivity and measurement of cytokines; A. P. and M. T. performed the adoptive transfer experiments. R. S. performed the flow cytometry analysis and immunohistochemistry; A. I., M. N. and G. C. performed the proliferation experiments; B. D'A and R. S. analysed the data.

Conflict of interest

None.

References

Alexander SPH, Benson HE, Faccenda E, Pawson AJ, Sharman JL, Spedding M *et al.* (2013a). The Concise Guide to PHARMACOLOGY 2013/14: G protein-coupled receptors. Br J Pharmacol 170: 1459–1581.

Alexander SPH, Benson HE, Faccenda E, Pawson AJ, Sharman JL, Spedding M *et al.* (2013b). The Concise Guide to PHARMACOLOGY 2013/14: Enzymes. Br J Pharmacol 170: 1797–1867.

Ammit AJ, Hastie AT, Edsall LC, Hoffman RK, Amrani Y, Krymskaya VP *et al.* (2001). Sphingosine 1-phosphate modulates human airway smooth muscle cell functions that promote inflammation and airway remodeling in asthma. FASEB J 15: 1212–1214.

Berrozpe G, Timokhina I, Yukl S, Tajima Y, Ono M (1999). The W(sh), W(57), and Ph Kit expression mutations define tissue-specific control elements located between -23 and -154 kb upstream of Kit. Blood 94: 2658–2666.

Bice JB, Leechawengwongs E, Montanaro A (2014). Biologic targeted therapy in allergic asthma. Ann Allergy Asthma Immunol 112: 108–115.

Cheng LE, Wang ZE, Locksley RM (2010). Murine B cells regulate serum IgE levels in a CD23-dependent manner. J Immunol 185: 5040–5047.

Chiba Y, Suzuki K, Kurihara E, Uechi M, Sakai H, Misawa M (2010). Sphingosine-1-phosphate aggravates antigen-induced airway inflammation in mice. Open Respir Med J 4: 82–85.

Finkelman FD, Holmes J, Katona IM, Urban JF Jr, Beckmann MP, Park LS *et al.* (1990). Lymphokine control of *in vivo* immunoglobulin isotype selection. Annu Rev Immunol 8: 303–333.

Galli SJ, Tsai M (2012). IgE and mast cells in allergic disease. Nat Med 18: 693–704.

Geha RS, Jabara HH, Brodeur SR (2003). The regulation of immunoglobulin E class-switch recombination. Nat Rev Immunol 3: 721–732.

Jenkins RW, Clarke CJ, Canals D, Snider AJ, Gault CR, Heffernan-Stroud L *et al.* (2011). Regulation of CC ligand 5/RANTES by acid sphingomyelinase and acid ceramidase. J Biol Chem 286: 13292–13303.

Kilkenny C, Browne W, Cuthill IC, Emerson M, Altman DG (2010). Animal research: Reporting *in vivo* experiments: the ARRIVE guidelines. Br J Pharmacol 160: 1577–1579.

Kume H, Takeda N, Oguma T, Ito S, Kondo M, Ito Y (2007). Sphingosine 1-phosphate causes airway hyper-reactivity by rho-mediated myosin phosphatase inactivation. J Pharmacol Exp Ther 320: 766–773.

Lai WQ, Wong WS, Leung BP (2011). Sphingosine kinase and sphingosine 1-phosphate in asthma. Biosci Rep 31: 145–150.

McGrath J, Drummond G, McLachlan E, Kilkenny C, Wainwright C (2010). Guidelines for reporting experiments involving animals: the ARRIVE guidelines. Br J Pharmacol 160: 1573–1576.

Metzger H (1991). The high affinity receptor for IgE on mast cells. Clin Exp Allergy 21: 269–279.

Morris SC, Lees A, Holmes JM, Jeffries RD, Finkelman FD (1994). Induction of B cell and T cell tolerance *in vivo* by anti-CD23 mAb. J Immunol 152: 3768–3776.

Olivera A (2008). Unraveling the complexities of sphingosine-1-phosphate function: the mast cell model. Prostaglandins Other Lipid Mediat 86: 1–11.

Olivera A, Rivera J (2011). An emerging role for the lipid mediator sphingosine-1-phosphate in mast cell effector function and allergic disease. Adv Exp Med Biol 716: 123–142.

Oskeritzian CA, Milstien S, Spiegel S (2007). Sphingosine-1-phosphate in allergic responses, asthma and anaphylaxis. Pharmacol Ther 115: 390–399.

Pawson AJ, Sharman JL, Benson HE, Faccenda E, Alexander SP, Buneman OP *et al.*; NC-IUPHAR (2014). The IUPHAR/BPS Guide to PHARMACOLOGY: an expert-driven knowledgebase of drug targets and their ligands. Nucl Acids Res 42 (Database Issue): D1098–D1106.

Price MM, Oskeritzian CA, Falanga YT, Harikumar KB, Allegood JC, Alvarez SE *et al.* (2012). A specific sphingosine kinase 1 inhibitor attenuates airway hyperresponsiveness and inflammation in a mast cell-dependent murine model of allergic asthma. J Allergy Clin Immunol 131: 501–511.

Pyne S, Pyne N (2000). Sphingosine 1-phosphate signalling via the endothelial differentiation gene family of G-protein-coupled receptors. Pharmacol Ther 88: 115–131.

Pyne S, Pyne NJ (2002). Sphingosine 1-phosphate signalling and termination at lipid phosphate receptors. Biochim Biophys Acta 1582: 121–131.

Rega A, Terlizzi M, Luciano A, Forte G, Crother TR, Arra C *et al.* (2013). Plasmacytoid dendritic cells play a key role in tumor progression in lipopolysaccharide-stimulated lung tumor-bearing mice. J Immunol 190: 2391–2402.

Rivera J, Fierro NA, Olivera A, Suzuki R (2008). New insights on mast cell activation via the high affinity receptor for IgE. Adv Immunol 98: 85–120.

Rosenwasser LJ (2011). Mechanisms of IgE inflammation. Curr Allergy Asthma Rep 2: 178–183.

Rosenwasser LJ, Meng J (2005). Anti-CD23. Clin Rev Allergy Immunol 29: 61–72.

Roviezzo F, Del Galdo F, Abbate G, Bucci M, D'Agostino B, Antunes E *et al*. (2004). Human eosinophil chemotaxis and selective *in vivo* recruitment by sphingosine 1-phosphate. Proc Natl Acad Sci U S A 101: 11170–11175.

Roviezzo F, Di Lorenzo A, Bucci M, Brancaleone V, Vellecco V, De Nardo M *et al*. (2007). Sphingosine-1-phosphate/sphingosine kinase pathway is involved in mouse airway hyperresponsiveness. Am J Respir Cell Mol Biol 36: 757–762.

Roviezzo F, D'Agostino B, Brancaleone V, De Gruttola L, Bucci M, De Dominicis G *et al*. (2010). Systemic administration of sphingosine-1-phosphate increases bronchial hyperresponsiveness in the mouse. Am J Respir Cell Mol Biol 42: 572–577.

Ryan JJ, Spiegel S (2008). The role of sphingosine-1-phosphate and its receptors in asthma. Drug News Perspect 21: 89–96.

Sorrentino R, Sukkar MB, Sriskandan S, Chung KF, Mitchell JA (2008). Differential regulation of CCL-11/eotaxin-1 and CXCL-8/IL-8 by gram-positive and gram-negative bacteria in human airway smooth muscle cells. Respir Res 1: 9–30.

Sorrentino R, Morello S, Forte G, Montinaro A, De Vita G, Luciano A (2011). B cells contribute to the antitumor activity of CpG-oligodeoxynucleotide in a mouse model of metastatic lung carcinoma. Am J Respir Crit Care Med 183: 1369–1379.

Spiegel S, Milstien S (2003). Sphingosine-1-phosphate: an enigmatic signalling lipid. Nat Rev Mol Cell Biol 4: 397–407.

Tono T, Tsujimura T, Koshimizu U, Kasugai T, Isozaki K, Nishikawa S *et al*. (1992). c-kit Gene was not transcribed in cultured mast cells of mast cell-deficient Wsh/Wsh mice that have a normal number of erythrocytes and a normal c-kit coding region. Blood 80: 1448–1453.

Zurawski G, de Vries JE (1994). Interleukin 13, an interleukin 4-like cytokine that acts on monocytes and B cells, but not on T cells. Immunol Today 15: 19–26.

Supporting information

Additional Supporting Information may be found in the online version of this article at the publisher's web-site:

http://dx.doi.org/10.1111/bph.13033

Figure S1 CD4+ T-cells were harvested from vehicle-, S1P-, IgG-anti-CD23, anti-CD23+ S1P-treated mice. CD4+ T-cells were cultured for 3 days in the presence or not of CD3/CD28 stimulating beads. Data represent mean ± SEM, $n = 5$. Experiments were performed on two different experimental days. Statistically significant differences are denoted by ** and *** indicating $P < 0.01$ and $P < 0.001$, respectively, as determined by Student's two-tailed *t*-test.